

Parallel Accumulation–Serial Fragmentation (PASEF): Multiplying Sequencing Speed and Sensitivity by Synchronized Scans in a Trapped Ion Mobility Device

Florian Meier,[†] Scarlet Beck,[†] Niklas Grassl,[†] Markus Lubeck,[‡] Melvin A. Park,[§] Oliver Raether,[‡] and Matthias Mann^{*,†}

[†]Proteomics and Signal Transduction, Max-Planck-Institute of Biochemistry, Am Klopferspitze 18, 82152 Martinsried, Germany

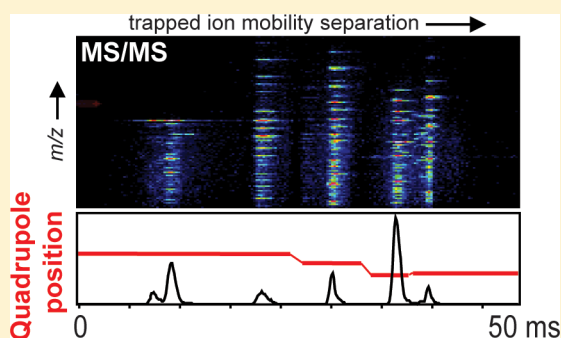
[‡]Bruker Daltonik GmbH, Fahrenheitstrasse 4, 28359 Bremen, Germany

[§]Bruker Daltonics Inc., 40 Manning Road, Billerica, Massachusetts 01821, United States

Supporting Information

ABSTRACT: In liquid chromatography-mass spectrometry (LC-MS)-based proteomics, many precursors elute from the column simultaneously. In data-dependent analyses, these precursors are fragmented one at a time, whereas the others are discarded entirely. Here we employ trapped ion mobility spectrometry (TIMS) on an orthogonal quadrupole time-of-flight (QTOF) mass spectrometer to remove this limitation. In TIMS, all precursor ions are accumulated in parallel and released sequentially as a function of their ion mobility. Instead of selecting a single precursor mass with the quadrupole mass filter, we here implement synchronized scans in which the quadrupole is mass positioned with sub-millisecond switching times at the m/z values of appropriate precursors, such as those derived from a topN precursor list. We demonstrate serial selection and fragmentation of multiple precursors in single 50 ms TIMS scans. Parallel accumulation–serial fragmentation (PASEF) enables hundreds of MS/MS events per second at full sensitivity. Modeling the effect of such synchronized scans for shotgun proteomics, we estimate that about a 10-fold gain in sequencing speed should be achievable by PASEF without a decrease in sensitivity.

KEYWORDS: proteomics, MS/MS, ion mobility, TIMS, peptide sequencing, multiplexing, time-of-flight, high resolution



INTRODUCTION

High-resolution mass spectrometry (MS)-based proteomics has emerged as a powerful technique for large-scale profiling of thousands of proteins with many applications in molecular and cellular biology.^{1–3} A typical bottom-up shotgun proteomics workflow starts with the extraction and solubilization of the protein material prior to enzymatic digestion. The peptide mixture is subsequently separated via liquid chromatography (LC) and electrosprayed into a mass spectrometer. To derive sequence information, suitable precursor ions are isolated by their mass-to-charge ratio (m/z) and subjected to collision-induced fragmentation, followed by database identification. Precursor scan and fragmentation are commonly performed with a data-dependent topN method, in which a MS survey spectrum is followed by fragmentation spectra of the N most abundant precursors. In complex mixtures, the depth of the analysis is thus foremost limited by the sequencing speed and sensitivity of the mass spectrometer. Previously we demonstrated that only 16% out of 100,000 peptide features eluting during a 90 min LC gradient were targeted for MS/MS.⁴ State-of-the-art proteomics MS instruments partly address these challenges by increasing sequencing speed and resolving

power.^{5,6} However, as more and more MS/MS spectra are acquired per second, less and less acquisition time is available for each precursor—an inherent consequence of the serial nature of the MS/MS process. Parallel fragmentation of unselected precursors in methods such as MS^{E7} or SWATH⁸ addresses this problem at the expense of multiplexing the MS/MS spectra, making peptide identification more challenging and precluding iTRAQ⁹ and TMT¹⁰ based multiplexing.^{10,11}

Time-of-flight (TOF) instruments acquire spectra at very high frequency. This makes them capable of using the majority of the precursor and fragment ions, thus promising optimal sensitivity and sequencing rates. However, although MS/MS rates of up to 100 Hz¹² can be readily achieved, in proteomic practice, sensitivity is generally not sufficient to detect an adequate number of fragment ions for peptide identification at such high scan speeds. That is, because the quadrupole filter transmits a given type of precursor ion for only a small fraction of the time in which that species is eluting from the LC column, only a small fraction of available precursor ions are utilized

Received: October 6, 2015

Published: November 5, 2015

when operating at high MS/MS spectral rates. Nevertheless, quadrupole TOF instruments have improved their performance over the last few years, and appear ready to become a viable alternative to the prevalent Orbitrap analyzer-based technology.^{13–16} We recently described a state of the art QTOF instrument, with high resolution and ion transmission, which enabled rapid and in-depth analysis of complex proteomes, including the identification of more than 11,000 different proteins in brain tissue.¹⁷

Due to their high scanning speeds (about 0.1 ms/spectrum), TOF instruments are compatible with ion mobility spectrometry (IMS), which happens on the time scale of tens of milliseconds.^{18–21} While IMS-MS can increase speed, selectivity, and sensitivity,^{22–24} available platforms have entailed a considerable increase in instrumental complexity and reduced ion transmission.²⁵ A particular form of ion mobility, termed trapped ion mobility spectrometry (TIMS), features a particularly compact construction, without compromising resolution or transmission.^{26–29} In the TIMS device, ions are accumulated in an RF-only tunnel at a position where the force of a gas flow equals the opposing force of an electric field. Ion mobility separated species are released from the device as a function of their collisional cross section. Here we asked if this sequential release after parallel accumulation can be exploited to drastically increase the speed and sensitivity of MS/MS experiments.

MATERIALS AND METHODS

Sample Preparation

Purified and predigested standards of enolase, phosphorylase b, alcohol dehydrogenase (ADH), and bovine serum albumin (BSA) were purchased from Waters GmbH (Eschborn, Germany) and resuspended in 0.1% formic acid to prepare stock solutions at a concentration of 10 pmol/ μ L each. These stock solutions were combined in an equimolar ratio and diluted in 50% water/50% acetonitrile/0.1% formic acid (v/v/v) to a final concentration of 100 fmol/ μ L.

Trapped ion mobility spectrometry–mass spectrometry

To mimic conditions during the analysis of complex proteomics samples, we directly infused the digested four protein mixture into a prototype, high-resolution QTOF mass spectrometer equipped with a TIMS device (flow rate 3 μ L/min). For an overview of the instrument, see the [Results and Discussion](#) below. A detailed description of the construction and operation of the TIMS analyzer employed here has been published elsewhere.^{26,30} Briefly, the TIMS device is composed of stacked ring electrodes, which form three distinct sections: an entrance funnel, the TIMS tunnel, and an exit funnel. The experiments were performed using nitrogen as a bath gas at room temperature, and the gas flow velocity was kept constant by regulating the pressure at the inlet and the outlet of the TIMS cartridge. Ions were accumulated for 50 ms, and mobility separation was achieved by ramping the entrance potential from -180 V to -40 V within 50 ms (435 TOF scans of 115 μ s each). TIMS and MS operation were controlled and synchronized using the instrument control software otofControl (Bruker Daltonik, Bremen, Germany).

Synchronized TIMS and quadrupole operation

To enable the PASEF method, precursor m/z and mobility information was first derived from full scan TIMS-MS experiments (with a mass range of m/z 150–1850). Resulting

quadrupole mass, collision energy, and switching times were manually transferred to the instrument controller as a function of the total cycle time via direct firmware commands. The quadrupole isolation width was set to 3 Th and, for fragmentation, the collision energies were varied between 30 and 60 eV depending on precursor mass and charge.

Data analysis and modeling of increased sequencing rates

Ion mobility resolved mass spectra, nested ion mobility vs m/z distributions, as well as summed fragment ion intensities were extracted from the raw data files with a prototype version of DataAnalysis (Bruker Daltonik). S/N ratios were increased by summations of individual TIMS scans. Mobility peak positions and peak half-widths were determined based on extracted ion mobilograms (± 0.05 Da) with an in-house script written in Python, using the peak detection algorithm implemented in the DataAnalysis software.

To model the anticipated benefit from PASEF scans for shotgun proteomics, we reanalyzed a single shot HeLa experiment from our recently published data set acquired on an impact II QTOF instrument.¹⁷ Feature detection and peptide identification were performed with MaxQuant version 1.5.2.8 applying the previously described search parameters. Further analysis of the MaxQuant output was performed in the R statistical computational environment.³¹ For each isotope pattern (“MS feature”), MaxQuant reports the minimum and maximum scan number where it was detected.³² To simulate a topN method, each detected feature was assigned to a single scan (at the minimum scan number) and the N most abundant features of each bin were selected according to the original MS peak picking criteria ($m/z > 300$ and charge > 1). This procedure reproduced the actual peak picking procedure performed by the Bruker acquisition software.

To restrict the simulations to likely peptide precursors, the MS features present in the MaxQuant output, as well as the target species assigned as described above, were further filtered for retention times between 10–100 min, charge state 2–5 and m/z values > 450 , which yielded a log-normal intensity distribution.

RESULTS AND DISCUSSION

Trapped ion mobility spectrometry (TIMS) – Mass spectrometry

To investigate the PASEF method that is the subject of this study, we made use of a prototype TIMS-QTOF mass spectrometer (Figure 1). In this instrument, a TIMS tunnel was incorporated into the first pumping stage, upstream from the transfer and selection quadrupoles and the high resolution mass analyzer.

Briefly, ions are generated in an electrospray source, transferred into the vacuum system through a glass capillary, deflected by 90°, and focused by the entrance funnel into the TIMS tunnel. This tunnel consists of pairs of stacked electrodes to which an RF field is applied. A DC field in the longitudinal direction is superimposed on this RF field (Figure 1B). Gas originating from the capillary flows through the sealed tunnel at a pressure of about 2–3 mbar. Ions entering the tunnel experience a drag due to the gas flow and a counteracting electrical field. They come to rest at a position where these two forces are equal and are radially confined by the pseudopotential induced by the RF field. Since the drag is proportional to the collisional cross section, ions of different mobility are trapped at different positions along the longitudinal axis, with

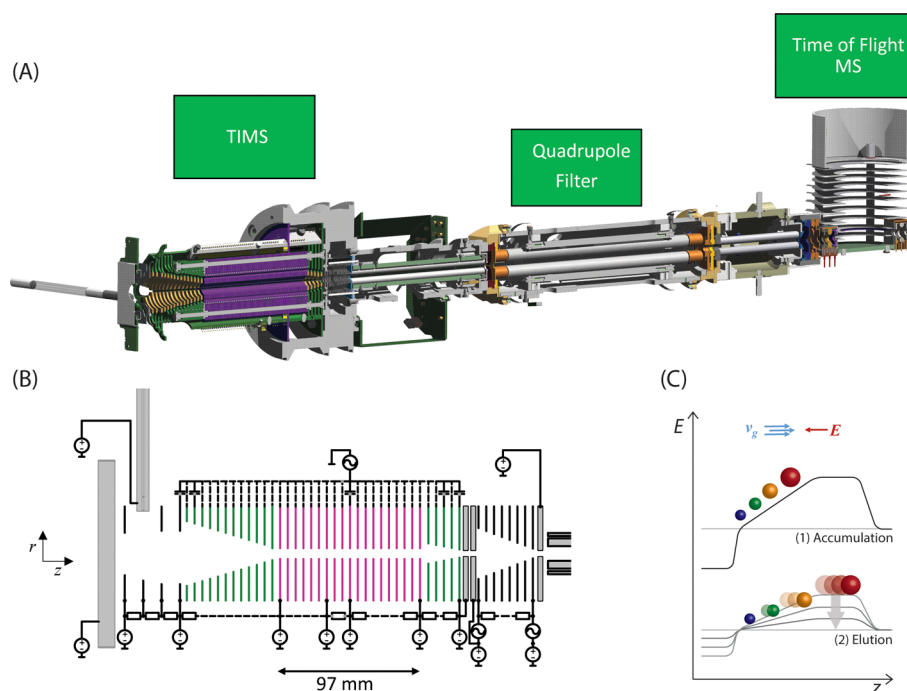


Figure 1. Trapped ion mobility spectrometry coupled to a QTOF mass spectrometer. (A) Instrument schematic of the prototype TIMS-QTOF instrument used in this study. (B) Detailed schematic of the TIMS tunnel (purple), enclosed by the entrance and exit funnels (green). (C) General mode of TIMS operation, including ion accumulation (1) and serial elution (2) of ion mobility separated ions from the TIMS device by decreasing the electrical field. The directed forces of the gas flow and electrical field are indicated by v_g and E .

high mobility ions at the entrance and low mobility ions near the exit of the tunnel (Figure 1C). After a desired ion accumulation time, further ions are prevented from entering the tunnel by a change of the potential on the deflection plate. Stored ions are then “eluted” by decreasing the electric field strength. Eluted ions are focused by the exit funnel and pass through a second funnel and transfer quadrupole. Precursor ions can be isolated by the analytical quadrupole mass filter for optional subsequent fragmentation in the collision cell. Afterward narrow ion packages are accelerated into a field-free drift region by the orthogonal deflection unit. A two-stage reflectron compensates differences in the kinetic energy of the ions and they are detected on an MCP detector coupled to a 10-bit digitizer, similar to the Bruker impact II instrument.¹⁷

The total length of the TIMS device is only about 10 cm (Figure 1B), and it is operated with modest potentials of less than 300 V. Since the resolution is mainly determined by the rate at which the electrical field is decreased, the user is free to adjust it based on experimental needs. For slow ramp times, ion mobility resolutions (expressed as $R = \Omega/\Delta\Omega$, where Ω is the collisional cross-section) of more than 200 have been demonstrated^{28,29} and faster scan out times of about 50 ms still allow $R > 40$.³⁰

Parallel accumulation–serial fragmentation (PASEF)

Ion mobility–mass spectrometry adds an additional dimension of separation to the standard MS scans. The elution ramp described above defines a complete cycle of TIMS-MS, with the ions that have the lowest mobility (largest collisional cross sections) in relation to their charge state passing through the instrument first. During the elution ramp, TOF spectra are recorded at high frequency (~ 8.7 kHz). We term the data structure generated during a TIMS-MS cycle a “TIMS scan”. Several TIMS scans can be added to obtain a TIMS-MS spectrum of a desired signal-to-noise.

The TOF spectra from one scan can be summed (i.e., projected onto the m/z axis) to determine the m/z and intensity of all the ions present. This information can then be used to create a topN target list for fragmentation. MS/MS is performed in the usual way by setting the quadrupole transmission window to the values in the topN list and applying the collision energy that is optimal for the precursor mass and charge state. The MS/MS spectra produced when incorporating ion mobility are similar in most respects to those obtained by MS/MS only, with two principal differences: First, compared to operation without IMS, in which the signal is recorded continuously as long as the precursor is selected, the signal is compressed into a short time—i.e. the duration of the mobility peak. This leads to better signal-to-noise as signal is concentrated whereas noise is distributed. Second, the different precursors present in the quadrupole selection window are separated from each other by their different ion mobilities even at the same m/z . This alleviates the ‘Precursor Ion Fraction (PIF) problem’, which comes about because PIF values are much smaller than one for a majority of precursors in proteomics experiments.^{4,33}

Despite these two advantages, MS/MS experiments performed in the above-described way still only make use of one selection window per scan, in common with all methods that use a mass selecting quadrupole to isolate precursors (Figure 2, upper panel). Inspired by the controllable nature of the release of ions from the TIMS device and the fact that cross sections roughly correlate with precursor mass,³⁴ we wondered if it would be possible to utilize several precursors in one scan, without giving up the mass selection of each of them by the quadrupole. In the PASEF method described and demonstrated here, the quadrupole is positioned at the m/z of a precursor eluting from the TIMS analyzer and is then rapidly moved to the next one as soon as it has eluted (Figure 2, lower panel). In

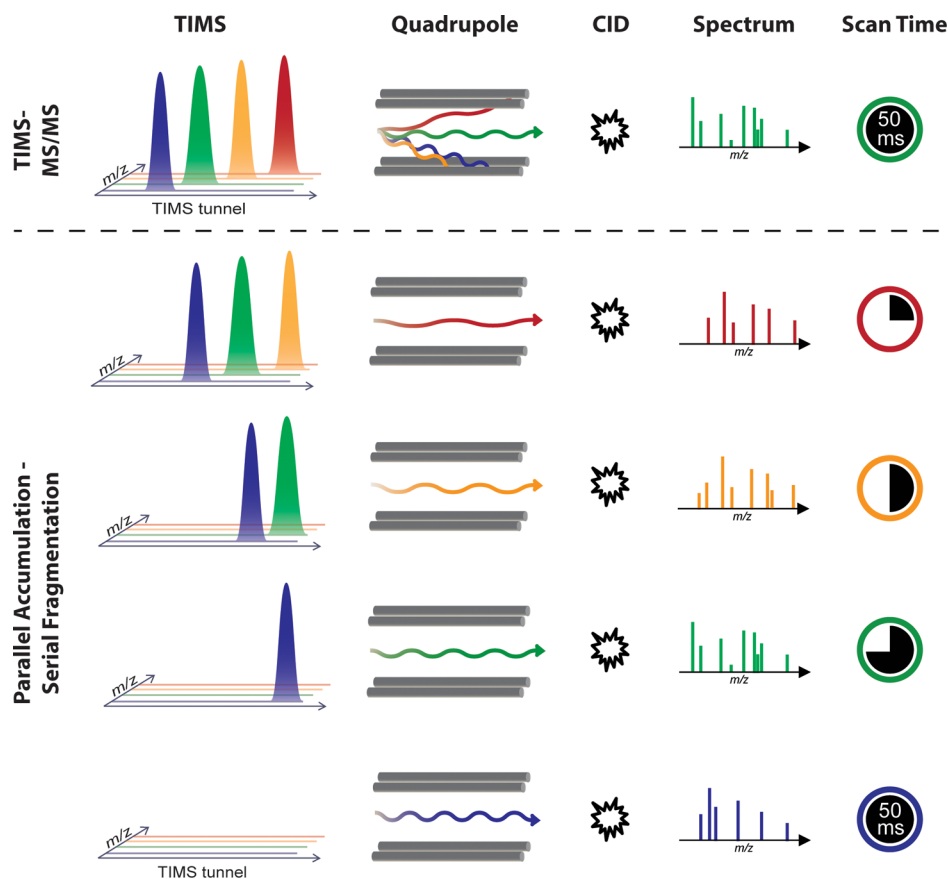


Figure 2. Illustration of the PASEF method in comparison with the standard TIMS-MS/MS operation mode. The top panel shows the selection of one precursor from a single TIMS scan, while all others are discarded. Conversely, the PASEF method (bottom panel) involves rapid switching of the quadrupole mass position to select multiple precursors at different m/z on the very same time scale. In this case, all targeted ions are fully used for fragmentation.

this way, the full intensity of the precursors that have been accumulated together can be utilized in one TIMS scan. This increases the speed of MS/MS by the number of precursors that are targeted. Alternatively, the same precursors can be selected in different TIMS scans to gain sensitivity; again by a factor up to the number of selected precursors per TIMS scan, or speed and sensitivity advantages can be combined as desired.

Time scales and required switching times

Key to realizing the concept of PASEF are the efficient storage of ions of the intended precursor range, high ion mobility resolution, and the extremely rapid switching of the quadrupole between precursors on the time scale of a single TIMS scan. To establish the hardware requirements for this, it is worthwhile to first consider the time scales of the individual processes involved in the LC-MS/MS experiment. With the QTOF setup in our laboratory,¹⁷ we typically achieve average chromatographic peak widths of about 7 s (FWHM) during a 90 min LC gradient. The MS acquisition cycle for a data-dependent top17 method is completed within 1.2 to 1.4 s. Given a 200 ms interval for summing MS survey scans of 110 μ s each, up to 17 precursors per second are selected by the quadrupole mass filter and fragmented in the collision cell. Therefore, the quadrupole mass position, as well as the collision energy, are switched every 60 ms. During this time, the TOF mass analyzer performs about 550 scans.

When incorporating ion mobility separation into this workflow, it becomes evident that a typical TIMS scan of 20

to 60 ms is orders of magnitude shorter than either the chromatographic peak widths or the topN cycle times (Figure 3). Conversely, the TIMS scan is about 100-fold longer than the time required for a single TOF scan and thus readily fits in between the chromatographic time scale and the TOF scan time. Individual ion mobility peaks have half widths of one millisecond or less (see below). Since the PASEF method aims to select multiple precursors from a single TIMS scan, precursor isolation should also happen within one millisecond. Note that this requires a much faster precursor isolation than the 60 ms of the normal top17 method, ideally by about 100-fold. To investigate the feasibility of quadrupole switching at these time scales, we first evaluated the rise times of the power supplies and lag times that potentially affect ion transmission. This revealed that the quadrupole is in principle capable of stepping its mass position by 3000 Th within 1.5 ms or less. Considering the much narrower m/z range relevant for proteomics, this should make even sub-millisecond switching times possible. Adding the width of a typical ion mobility peak results in a quadrupole isolation time per precursor of currently 2.5 to 4 ms. This translates into a maximum of 12–20 precursors per 50 ms TIMS scan, or 240–400 precursors per second. Importantly, the signal per precursor still corresponds to the full accumulation time. Thus, PASEF should be able to measure MS/MS spectra up to 12–20 times faster without losing sensitivity. Clearly, this number exceeds the number of precursors that can usefully be selected for fragmentation in contemporary shotgun proteomics experiments. Therefore,

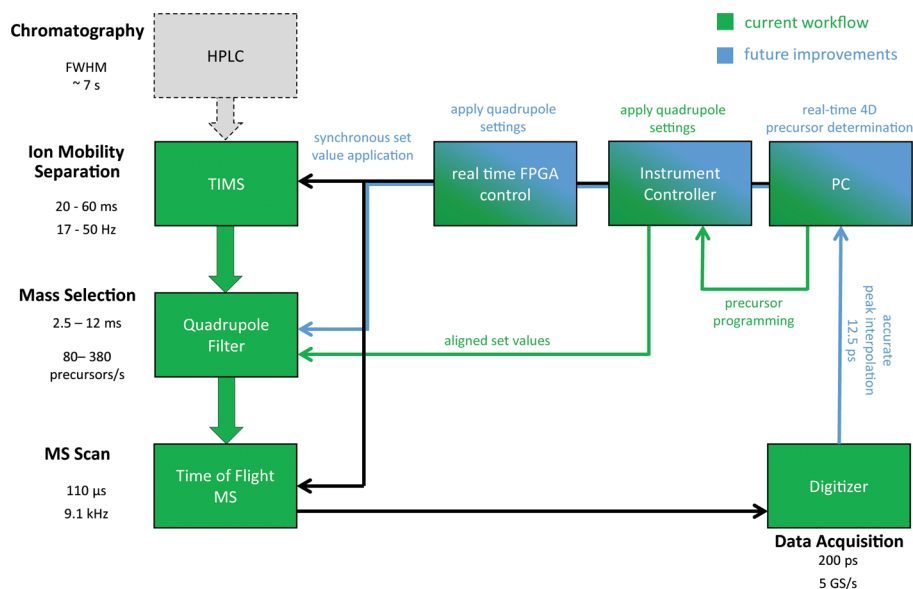


Figure 3. Investigation of hardware requirements for the PASEF method, including time scales and switching times of a typical proteomics LC-TIMS-MS/MS experiment. Arrows and lines visualize the hardware connections in the currently used setup (green) and planned future improvements (blue). GS/s, Giga-samples per second.

excess sequencing speed can be expended on improving identification scores or MS/MS-based quantification as explained in more detail below.

Precursor selection at this frequency can also be limited by the rate at which the quadrupole set values are calculated and applied by the instrument controller. In fact, we found this to be one of the major bottlenecks of our current setup since the set values are transferred via a comparably slow serial interface, precluding a fully synchronized operation of the quadrupole and TIMS. For our proof of principle experiments, we here circumvent this limitation by determining the elution times from TIMS precursor scans and applying the mass position and switching times for MS/MS scans to the quadrupole via the instrument controller in an asynchronous manner. This enabled us to select four precursors for a single TIMS scan. In the future, we will overcome this limitation by moving the calculations and set value application to the real time field-programmable gate array (FPGA), which already synchronizes TIMS and TOF analyzer. An additional direct interface to the quadrupole driver will allow set value applications in less than 50 μs, thus no longer compromising the quadrupole switching times (depicted in blue in Figure 3).

Note that the PASEF operation performed here will not change due to these improvements, except that we will be able to make use of the maximum mass selection rate of the quadrupole. Moreover, advanced peak detection and compression algorithms executed by the digitizer, capable of handling several million peaks per second, will enable real-time precursor determination in four dimensions (LC retention time, elution time from the TIMS device, m/z value and intensity) as required for data-dependent topN methods. To not compromise the proteome coverage in a shotgun experiment, this will also involve dynamic exclusion of already sequenced peptides. However, as the precursor determination itself can take up to a few milliseconds, we plan to parallelize precursor search and data acquisition. Notably, this strategy would also support more sophisticated precursor search algorithms without reducing the duty cycle for data acquisition. From

the discussion above, we conclude that current limitations are not of a fundamental nature, but tasks for engineering and data-handling which are likely to be accomplished in the near future.

Application of PASEF to complex protein digests

Having established sub-millisecond switching of the quadrupole isolation window, we next aimed to examine the novel method under circumstances that mimic the simultaneous elution of many peptides from the chromatographic column in shotgun proteomics. We thus directly infused an unseparated mixture of digested ADH, BSA, enolase and phosphorylase b to generate high peptide complexity (Materials and Methods).

Figure 4A shows the result of an ESI-TIMS-MS analysis of the four protein mixture. Without ion mobility separation, this experiment would have yielded a very complex mass spectrum with multiple overlapping signals as indicated by the projection on the m/z axis on the right. TIMS separates these overlapping ion species by their mobility, resulting in much less complex mass spectra per TOF scan. In accordance with others,^{19,35} we observe a significant correlation between m/z and mobility, whereas higher m/z species are less mobile and vice versa. There are two main populations that can be assigned to different charge states, with singly charged species being less mobile than their multiply charged counterparts at similar m/z . Charge 2–5 species—potential tryptic peptides—make up a more dense population. Nevertheless, close inspection of the mobility peak widths in this regime revealed that the elution time chosen (ramping down the TIMS tunnel gradient in 50 ms) was sufficient to achieve a mobility resolution above 40 and to separate these species.

From the heat map created by the multiply charged tryptic peptides of the protein mixture, we first selected four mobility separated precursors. Corresponding mass positions at m/z 810.3 (1), 714.3 (2), 559.3 (3) and 560.6 (4) and the appropriate switching times were uploaded to the instrument controller. As apparent from Figure 4B, the quadrupole correctly isolated these precursors on the TIMS time scale. In each case, the entire peak was quantitatively captured. Projection onto the m/z scale also shows successful isolation,

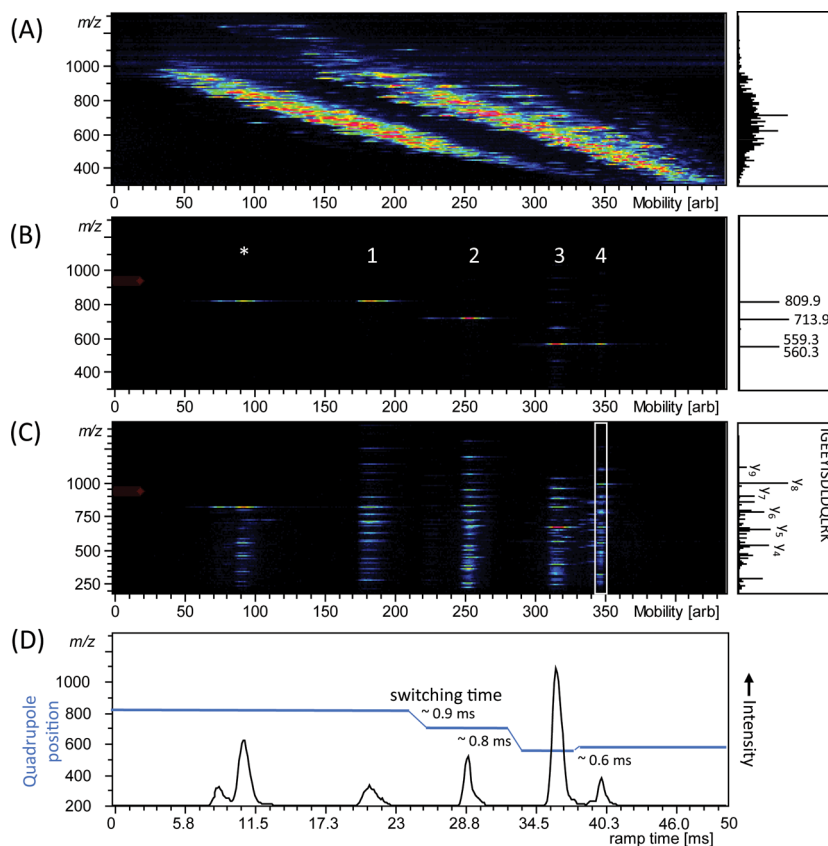


Figure 4. TIMS-QTOF analysis of electrosprayed peptides from a combined tryptic digest of ADH, BSA, phosphorylase b, and enolase. (A) Nested m/z and ion mobility distribution as detected in full scan MS. (B) Sequential isolation of four ions at different m/z that are separated by mobility after parallel accumulation. (C) Parallel accumulation–serial fragmentation (PASEF) of the precursors as isolated in (B). (D) Arrival time distribution of the summed fragment ions as observed by the PASEF method together with the quadrupole isolation mass as a function of the TIMS ramp time. Projected mass spectra are shown on the right of the panels, in (C) the fragments of the white box are projected.

and comparison to the spectrum without quadrupole isolation demonstrates a drastic simplification of the precursor population. Precursors (3) and (4) only differ in one m/z unit, representing the classical PIF problem, but are clearly separated by the combination of ion mobility and quadrupole isolation. Another notable feature is the peak isolated before peptide (1) and marked with an asterisk. This is caused by the fact that in the current configuration the quadrupole immediately started selection from the first m/z value. Consequently, it isolated a precursor from the singly charged population, which is widely separated from the actual target and upon inspection turns out to consist of two species that are distinct in mass and ion mobility.

In the next step, we applied the PASEF method by performing MS/MS on the isolated precursors. This led to a characteristic ladder of fragment ions at each precursor (Figure 4C, Supplementary Figure S1). Projection of the ladder generated by peptide (4) shows a standard MS/MS spectrum, corresponding to the sequence IGEEISDLQLRK from phosphorylase B. The other peptides corresponded to VLGI-DGGEGKEELFR (1) from enolase, HLQIYEINQR (2) from phosphorylase B and VAAAFPGDVDR (3), also from phosphorylase B. Interestingly, we were also able to assign one of the singly charged species to ADH based on its peptide fragment spectrum (YVVDTSK). Projection of all fragment ions onto the ion mobility axis shows coherence in arrival times, with fragment ion distributions very similar to their precursors (Figure 4D). These peaks were less than 3 ms wide, with typical

half-widths of around 1 ms. In contrast, the chosen quadrupole isolation times were at least three times longer and could therefore in principle have been shortened considerably. Combined with the fast switching times apparent in the figure, this shows that at least ten precursors could have been targeted in this 50 ms ramp.

To demonstrate PASEF on a larger scale, we extended the previously described experiment to a total of ten sets of four precursors each. The results on the 40 precursors were very similar to the example discussed above and are summarized in Table 1. The selected precursors span a mass range from m/z 418 to 956 and exhibited ion mobilities corresponding to TIMS elution times between 17 and 44 ms with an average half width of 0.8 ± 0.2 ms. In this experiment we also quantified the gain due to PASEF by comparing it to standard fragmentation of the 40 precursors with TIMS. With full realization of the PASEF concept, we would expect that we would preserve full signal intensity despite being 4-fold faster (or N -fold in general, where N is the number of selected precursors). This was fully validated by the results, which showed a ratio indistinguishable from one between the two cases (0.94 ± 0.12 , Table 1).

Modeling of coverage improvements in shotgun proteomics

Having demonstrated that PASEF is capable of a four to more than 10-fold increase in MS/MS speed at full sensitivity, we next modeled the effect of such an improvement on typical shotgun proteomics data. We built on our previous analysis, in

Table 1. PASEF Analysis of 40 Precursors from a Complex Mixture of Four Digested Proteins

Scan	Precursor				Mobility	FWHM	Ratio
	Protein	Peptide Sequence Targeted	<i>m/z</i>	Charge	[ms]	[ms]	PASEF/TIMS ^a
1	Enolase	VLGIDGGEGKEELFR	809.956	2	22.6	1.3	0.87
	Phos b	HLQIYEINQR	713.897	2	30.4	0.7	0.85
	Phos b	VAAAFPGDVDR	559.253	2	37.4	0.9	0.97
	Phos b	IGEEYISDLLQLRK	560.261	3	40.9	0.5	0.96
2	Enolase	SIVPSGASTGVHEALEMR	921.033	2	17.4	1.3	0.95
	Phos b	IGEEYISDLLQLR	775.914	2	28.2	0.7	0.97
	BSA	LVNELTEFAK	582.292	2	36.2	0.7	0.77
	BSA	LFTFHADICTLPDTEK	636.633	3	39.6	1.1	0.90
3	Phos b	TCAYTNHTVLPEALER	938.031	2	22.0	1.5	0.94
	Phos b	VLYPNDNFFEGK	721.862	2	28.7	0.7	1.00
		<i>no match</i>	658.303	4	35.1	0.6	1.12
	Phos b	LITAIGDVVNHDVPVGDGR	630.659	3	39.7	0.9	1.00
4	Enolase	TAGIQIVADDLTVTNPK	878.527	2	23.2	0.7	1.07
		<i>no match</i>	767.925	2	29.8	0.9	0.93
	BSA	DAIPENLPPLTADFAEDKDVCK	820.099	3	34.2	0.7	1.10
	Phos b	TNFDAFPDK	527.705	2	40.3	0.6	0.82
5	Phos b	WLVLCNPGLAIEIAER	927.568	2	22.4	0.8	0.95
	Enolase	AVDDFLISLDGTANK	789.928	2	29.3	0.8	0.92
		<i>no match</i>	594.311	2	35.5	0.7	1.01
	Phos b	TCAYTNHTVLPEALER	625.624	3	39.9	0.9	0.82
6		<i>no match</i>	955.970	2	17.3	0.7	1.09
	Phos b	DFNVGGYIQAVLDR	783.927	2	27.6	0.8	0.91
	ADH	SISIVGSYVGNR	626.323	2	34.5	0.6	0.92
	Enolase	VLGIDGGEGKEELFR	540.249	3	39.0	0.8	0.92
7	BSA	YNGVFQECQAEDK	874.403	2	27.1	0.9	0.93
	Phos b	VFADYEEYVK	631.784	2	33.6	0.6	(0.37) ^b
	Phos b	QRLPAPDEK	527.248	2	37.5	0.8	0.90
	BSA	DDPHACYSTVFDK	518.847	3	43.4	0.6	0.72
8	Phos b	IGEEYISDLLQLRK	839.973	2	24.2	0.8	1.05
	ADH	GLAGVENVTELKK	679.383	2	31.4	0.8	1.04
	Phos b	ARPEFTLPVHFYGR	563.934	3	37.7	0.6	0.78
	ADH	IGDYAGIK	418.668	2	43.6	0.6	1.03
9	BSA	KVPQVSTPTLVEVSR	820.502	2	26.4	0.8	0.98
	Phos b	LLSYVDDEAFIR	720.877	2	30.2	1.0	0.88
	Phos b	VAIQLNDRTHPSLAPELMR	706.720	3	34.9	0.8	1.05
	Phos b	APNDFNLK	459.682	2	41.2	0.6	(0.28) ^b
10		<i>no match</i>	782.429	2	23.8	0.7	1.16
	BSA	HLVDEPQNLK	653.351	2	32.6	0.8	1.13
	Enolase	IGSEVYHNLK	580.281	2	35.3	0.7	0.67
	Phos b	NLAENISR	458.691	2	39.7	0.6	0.70

^aMedian summed fragment ion intensities were extracted for each precursor from PASEF ($N = 331$) and TIMS-MS/MS ($N = 9$) scans with identical quadrupole isolation settings. ^bAs an artifact resulting from the asynchronous operation of TIMS and quadrupole, these two precursors were not isolated in each PASEF scan.

which we used MaxQuant to determine the number of isotope patterns (“peptide features”) as a function of retention time in a 90 min analysis of a HeLa digest and used this to evaluate speed, sensitivity and separation power achievable in shotgun proteomics.⁴ We repeated this analysis using our data from the impact II QTOF instrument,¹⁷ on which our prototype is based (Materials and Methods). From the first to last eluting peptides, about 50 to 70 unique features/s are detected by MaxQuant, of which about 12 had been fragmented per second (Figure 5A). The 4-fold improvement in sequencing speed already demonstrated above would allow targeting 80% of all detected features. We noted above that a 10-fold improvement is entirely consistent with the actually achieved switching times and ion mobility resolution. This would result in a targeting rate of about 125 features/s, far above the number of features

detected in the previous data set. That said, adding ion mobility could be expected to increase the number of resolvable peptide features in shotgun proteomics runs, in which case even a 10-fold increased sequencing speed could in principle be used entirely on unique peptide features.

However, not all detected features are suitable for MS/MS fragmentation because their peptide intensity may be too low to result in useful MS/MS spectra. Redoing the peptide histogram analysis that we had done on the original Orbitrap data⁴ revealed 3-fold larger numbers for the impact II data set but the same proportions: About 250,000 peptide features can be detected in the 90 min gradient, of which about 45,000 were fragmented, and about 30,000 with attendant peptide identification (Figure 5B).

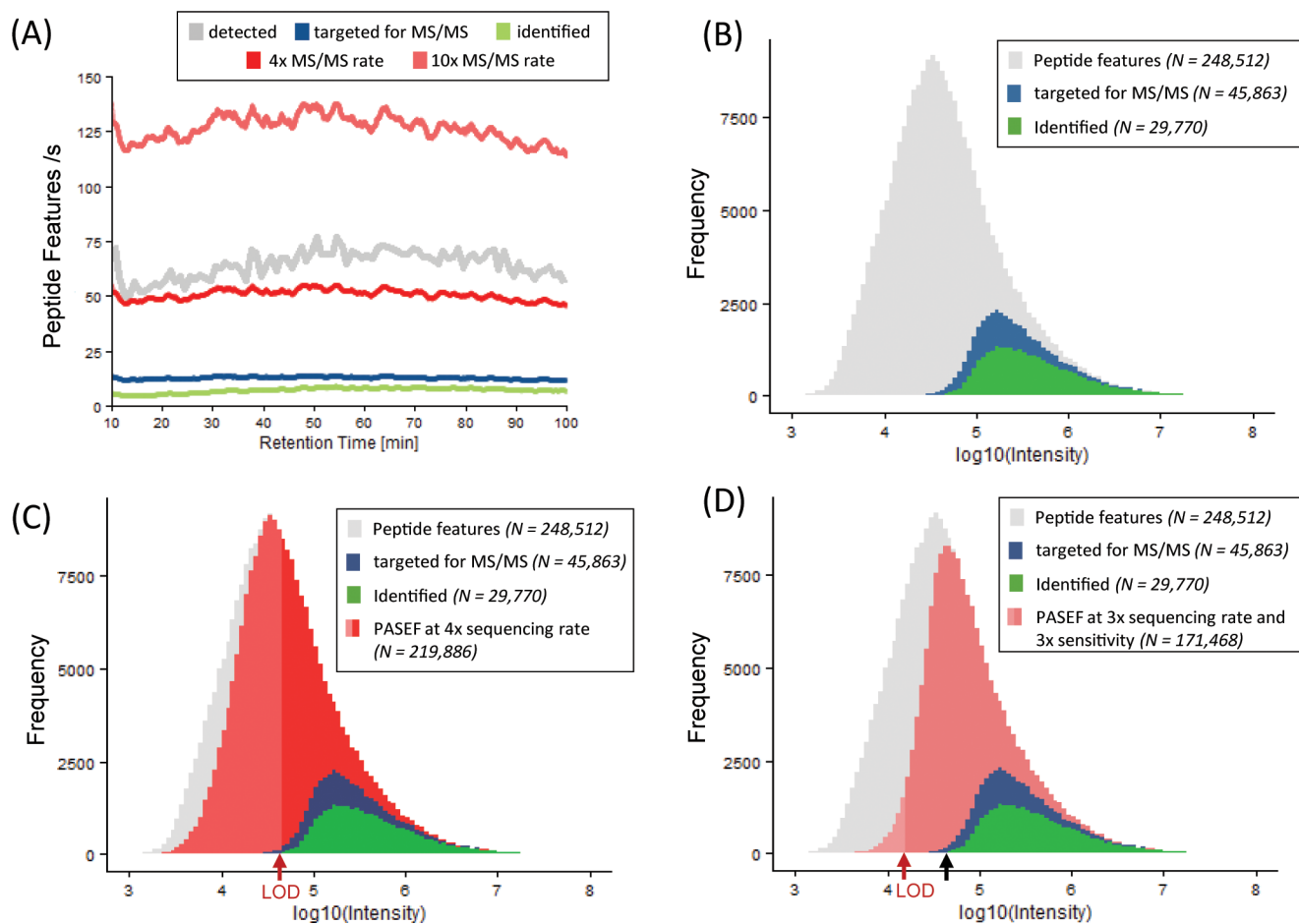


Figure 5. Modeling the benefits of the PASEF method in shotgun proteomics. (A) Peptide features per second eluting during a 90 min gradient. The gray trace indicates detected peptide features during conventional LC-MS/MS analysis of a tryptic HeLa digest on a QTOF instrument; blue and green traces indicate features that were targeted for MS/MS and successfully identified in the impact II data set.¹⁷ Red traces represent the simulated sequencing speed of PASEF with four and ten precursor ions per TIMS scan, respectively. (B) Intensity distribution of detected (gray), targeted (blue), and identified (green) peptide features extracted by MaxQuant from the impact II data set. (C) Same as (B) with a simulation of targeted peptides at 4-fold sequencing speed with the PASEF method (red). (D) Same as (B) with a simulation of a PASEF experiment with three precursors per scan and 3-fold increased sensitivity due to retargeting (red). MS features below the anticipated limit of detection (LOD) are indicated by reduced opacity.

With 4-fold higher sequencing speed, essentially the entire population of detected peptide features can now be targeted, but lower intensity precursors would diminish identification success (Figure 5C). The sensitivity of the impact II instrument for peptide identification is given by the lower limit of the green population in the peptide histogram. If we assume that the current instrument reaches at least the same sensitivity, then a 4-fold improvement in sequencing at full sensitivity, allows filling in about 40% of the entire peptide precursor population, a 250% improvement from before.

As mentioned above, the PASEF advantage could be used for increasing sequencing speed or sensitivity—through targeting the same feature repeatedly. In practice, we imagine that one would use a combination of both, for instance by fragmenting sufficiently abundant precursors once but summing MS/MS spectra for lower abundant ones. To model this in a simple way, we equally assigned the expected 10-fold improvement due to PASEF to sequencing speed and sensitivity gain (Figure 5D). This leads to a similarly shaped distribution of targeted precursor as in the experimental distribution, with the difference that the target and likely identified populations are increased by 300%. As a result, 70% of the overall precursor

population can now be targeted and potentially identified by MS/MS. Future experiments, using a full LC-TIMS-MS/MS set up, will reveal optimal combinations of refragmentation and precursors per TIMS scan. We also note that more sophisticated selection strategies for MS/MS could further improve the proportion of successfully identified peptides and that improvements in ion beam intensity would increase both the total number of detected features as well as the number of targetable and identifiable peptides.

CONCLUSIONS

Coupling ion mobility spectrometry to MS comprises several advantages, such as separation of ions from protein mixtures according to their size-to-charge ratio. Using the compact TIMS analyzer implemented into a state of the art QTOF mass spectrometer, we have here introduced the concept of PASEF. Sub-millisecond quadrupole switching times allowed us to select multiple precursors for fragmentation during a 50 ms ion mobility scan instead of only one. Importantly, we demonstrated that synchronized quadrupole and TIMS operation is fully quantitative in that the signal is not diminished compared to single precursor selection. An important advantage of PASEF

is that the resulting spectra—in addition to the ion mobility dimension—are fully precursor mass resolved, unlike recently proposed data independent strategies. This also makes PASEF compatible with reporter ion based chemical multiplexing strategies, such as iTRAQ or TMT. The about 10-fold gain that should be achievable by PASEF in shotgun proteomics experiments can be employed as increased sequencing speed without a decrease in sensitivity. However, modeling suggests that a combination of targeting more precursors and targeting weak precursors repeatedly, will be most effective. While demonstrated here for the TIMS-QTOF combination, the PASEF principle could be applied to any ion mobility–mass spectrometer configuration with the required sub-millisecond scan speed in the MS read out.

■ ASSOCIATED CONTENT

Supporting Information

The Supporting Information is available free of charge on the ACS Publications website at DOI: 10.1021/acs.jproteome.5b00932.

Supplementary Figure S-1: Annotated PASEF-MS/MS spectra of the peptides shown in Figure 4 (PDF)

■ AUTHOR INFORMATION

Corresponding Author

*Phone: +49-89-8578-2557. E-mail: mmann@biochem.mpg.de.

Author Contributions

All authors contributed to the research design; F.M., S.B., and M.L. performed research; F.M., S.B., M.L., O.R., and M.M. analyzed data; F.M., S.B., O.R., and M.M. wrote the manuscript. All authors have given approval to the final version of the manuscript. F.M. and S.B. contributed equally.

Notes

The authors declare the following competing financial interest(s): Several authors are employees of Bruker.

■ ACKNOWLEDGMENTS

We thank our colleagues in the Department of Proteomics and Signal Transduction and at Bruker for fruitful discussions. We particularly acknowledge our co-workers in Bremen, Niels Goedecke, Joerg Hoffmann, and Stefan Harsdorf, for support in setting up the prototype, as well as Peter Sander and Thomas Betz for providing data analysis tools. We acknowledge Max-Planck Society for the Advancement of Sciences for funding.

■ ABBREVIATIONS

ADH, alcohol dehydrogenase; BSA, bovine serum albumin; FPGA, field-programmable gate array; FWHM, full width at half-maximum; GS/s, Giga-samples per second; IM, ion mobility; LC, liquid chromatography; MS, mass spectrometry; MS/MS, tandem mass spectrometry; PASEF, parallel accumulation–serial fragmentation; PIF, precursor ion fraction; QTOF, quadrupole time-of-flight; RF, radiofrequency; TIMS, trapped ion mobility spectrometry; TOF, time-of-flight

■ REFERENCES

- (1) Aebersold, R.; Mann, M. Mass spectrometry-based proteomics. *Nature* **2003**, *422* (6928), 198–207.
- (2) Cravatt, B. F.; Simon, G. M.; Yates, J. R., 3rd. The biological impact of mass-spectrometry-based proteomics. *Nature* **2007**, *450* (7172), 991–1000.

- (3) Altaelaar, A. F.; Munoz, J.; Heck, A. J. Next-generation proteomics: towards an integrative view of proteome dynamics. *Nat. Rev. Genet.* **2013**, *14* (1), 35–48.

- (4) Michalski, A.; Cox, J.; Mann, M. More than 100,000 detectable peptide species elute in single shotgun proteomics runs but the majority is inaccessible to data-dependent LC-MS/MS. *J. Proteome Res.* **2011**, *10* (4), 1785–93.

- (5) Kelstrup, C. D.; Jersie-Christensen, R. R.; Batth, T. S.; Arrey, T. N.; Kuehn, A.; Kellmann, M.; Olsen, J. V. Rapid and Deep Proteomes by Faster Sequencing on a Benchtop Quadrupole Ultra-High-Field Orbitrap Mass Spectrometer. *J. Proteome Res.* **2014**, *13*, 6187.

- (6) Scheltema, R. A.; Hauschild, J. P.; Lange, O.; Hornburg, D.; Denisov, E.; Damoc, E.; Kuehn, A.; Makarov, A.; Mann, M. The Q Exactive HF, a Benchtop Mass Spectrometer with a Pre-filter, High-performance Quadrupole and an Ultra-high-field Orbitrap Analyzer. *Mol. Cell. Proteomics* **2014**, *13* (12), 3698–708.

- (7) Li, G. Z.; Vissers, J. P.; Silva, J. C.; Golick, D.; Gorenstein, M. V.; Geromanos, S. J. Database searching and accounting of multiplexed precursor and product ion spectra from the data independent analysis of simple and complex peptide mixtures. *Proteomics* **2009**, *9* (6), 1696–719.

- (8) Gillet, L. C.; Navarro, P.; Tate, S.; Rost, H.; Selevsek, N.; Reiter, L.; Bonner, R.; Aebersold, R. Targeted data extraction of the MS/MS spectra generated by data-independent acquisition: a new concept for consistent and accurate proteome analysis. *Mol. Cell. Proteomics* **2012**.

- (9) Ross, P. L.; Huang, Y. N.; Marchese, J. N.; Williamson, B.; Parker, K.; Hattan, S.; Khainovski, N.; Pillai, S.; Dey, S.; Daniels, S.; Purkayastha, S.; Juhasz, P.; Martin, S.; Bartlett-Jones, M.; He, F.; Jacobson, A.; Pappin, D. J. Multiplexed protein quantitation in *Saccharomyces cerevisiae* using amine-reactive isobaric tagging reagents. *Mol. Cell. Proteomics* **2004**, *3* (12), 1154–69.

- (10) Thompson, A.; Schafer, J.; Kuhn, K.; Kienle, S.; Schwarz, J.; Schmidt, G.; Neumann, T.; Johnstone, R.; Mohammed, A. K.; Hamon, C. Tandem mass tags: a novel quantification strategy for comparative analysis of complex protein mixtures by MS/MS. *Anal. Chem.* **2003**, *75* (8), 1895–904.

- (11) Wiese, S.; Reidegeld, K. A.; Meyer, H. E.; Warscheid, B. Protein labeling by iTRAQ: a new tool for quantitative mass spectrometry in proteome research. *Proteomics* **2007**, *7* (3), 340–50.

- (12) Andrews, G. L.; Simons, B. L.; Young, J. B.; Hawkridge, A. M.; Muddiman, D. C. Performance characteristics of a new hybrid quadrupole time-of-flight tandem mass spectrometer (TripleTOF 5600). *Anal. Chem.* **2011**, *83* (13), 5442–6.

- (13) Silva, J. C.; Denny, R.; Dorschel, C. A.; Gorenstein, M.; Kass, I. J.; Li, G. Z.; McKenna, T.; Nold, M. J.; Richardson, K.; Young, P.; Geromanos, S. Quantitative proteomic analysis by accurate mass retention time pairs. *Anal. Chem.* **2005**, *77* (7), 2187–200.

- (14) Silva, J. C.; Denny, R.; Dorschel, C.; Gorenstein, M. V.; Li, G. Z.; Richardson, K.; Wall, D.; Geromanos, S. J. Simultaneous qualitative and quantitative analysis of the *Escherichia coli* proteome: a sweet tale. *Mol. Cell. Proteomics* **2006**, *5* (4), 589–607.

- (15) Distler, U.; Kuharev, J.; Navarro, P.; Levin, Y.; Schild, H.; Tenzer, S. Drift time-specific collision energies enable deep-coverage data-independent acquisition proteomics. *Nat. Methods* **2014**, *11* (2), 167–70.

- (16) Helm, D.; Vissers, J. P.; Hughes, C. J.; Hahne, H.; Ruprecht, B.; Pachel, F.; Grzyb, A.; Richardson, K.; Wildgoose, J.; Maier, S. K.; Marx, H.; Wilhelm, M.; Becher, I.; Lemeer, S.; Bantscheff, M.; Langridge, J. I.; Kuster, B. Ion mobility tandem mass spectrometry enhances performance of bottom-up proteomics. *Mol. Cell. Proteomics* **2014**, *13*, 3709.

- (17) Beck, S.; Michalski, A.; Raether, O.; Lubeck, M.; Kaspar, S.; Goedecke, N.; Baessmann, C.; Hornburg, D.; Meier, F.; Paron, I.; Kulak, N. A.; Cox, J.; Mann, M. The Impact II, a Very High-Resolution Quadrupole Time-of-Flight Instrument (QTOF) for Deep Shotgun Proteomics. *Mol. Cell. Proteomics* **2015**, *14* (7), 2014–29.

- (18) Hoaglund, C. S.; Valentine, S. J.; Sporleder, C. R.; Reilly, J. P.; Clemmer, D. E. Three-dimensional ion mobility/TOFMS analysis of electrosprayed biomolecules. *Anal. Chem.* **1998**, *70* (11), 2236–42.

(19) Valentine, S. J.; Counterman, A. E.; Hoaglund, C. S.; Reilly, J. P.; Clemmer, D. E. Gas-phase separations of protease digests. *J. Am. Soc. Mass Spectrom.* **1998**, *9* (11), 1213–6.

(20) Kanu, A. B.; Dwivedi, P.; Tam, M.; Matz, L.; Hill, H. H., Jr. Ion mobility-mass spectrometry. *J. Mass Spectrom.* **2008**, *43* (1), 1–22.

(21) May, J. C.; McLean, J. A. Ion mobility-mass spectrometry: time-dispersive instrumentation. *Anal. Chem.* **2015**, *87* (3), 1422–36.

(22) Hoaglund-Hyzer, C. S.; Clemmer, D. E. Ion trap/ion mobility/quadrupole/time-of-flight mass spectrometry for peptide mixture analysis. *Anal. Chem.* **2001**, *73* (2), 177–84.

(23) Shliha, P. V.; Bond, N. J.; Gatto, L.; Lilley, K. S. Effects of traveling wave ion mobility separation on data independent acquisition in proteomics studies. *J. Proteome Res.* **2013**, *12* (6), 2323–39.

(24) Lanucara, F.; Holman, S. W.; Gray, C. J.; Evers, C. E. The power of ion mobility-mass spectrometry for structural characterization and the study of conformational dynamics. *Nat. Chem.* **2014**, *6* (4), 281–94.

(25) Cumeras, R.; Figueras, E.; Davis, C. E.; Baumbach, J. I.; Gracia, I. Review on ion mobility spectrometry. Part 1: current instrumentation. *Analyst* **2015**, *140* (5), 1376–90.

(26) Fernandez-Lima, F. A.; Kaplan, D. A.; Park, M. A. Note: Integration of trapped ion mobility spectrometry with mass spectrometry. *Rev. Sci. Instrum.* **2011**, *82* (12), 126106.

(27) Fernandez-Lima, F.; Kaplan, D. A.; Suetering, J.; Park, M. A. Gas-phase separation using a trapped ion mobility spectrometer. *Int. J. Ion Mobility Spectrom.* **2011**, *14* (2–3), 93.

(28) Silveira, J. A.; Ridgeway, M. E.; Park, M. A. High resolution trapped ion mobility spectrometry of peptides. *Anal. Chem.* **2014**, *86* (12), 5624–7.

(29) Ridgeway, M. E.; Silveira, J. A.; Meier, J. E.; Park, M. A. Microheterogeneity within conformational states of ubiquitin revealed by high resolution trapped ion mobility spectrometry. *Analyst* **2015**, *140* (20), 6964–72.

(30) Michelmann, K.; Silveira, J. A.; Ridgeway, M. E.; Park, M. A. Fundamentals of trapped ion mobility spectrometry. *J. Am. Soc. Mass Spectrom.* **2015**, *26* (1), 14–24.

(31) R Development Core Team. *R: A Language and Environment for Statistical Computing*; 2014.

(32) Cox, J.; Matic, I.; Hilger, M.; Nagaraj, N.; Selbach, M.; Olsen, J. V.; Mann, M. A practical guide to the MaxQuant computational platform for SILAC-based quantitative proteomics. *Nat. Protoc.* **2009**, *4* (5), 698–705.

(33) Houel, S.; Abernathy, R.; Renganathan, K.; Meyer-Arendt, K.; Ahn, N. G.; Old, W. M. Quantifying the impact of chimera MS/MS spectra on peptide identification in large-scale proteomics studies. *J. Proteome Res.* **2010**, *9* (8), 4152–60.

(34) Revercomb, H. E.; Mason, E. A. Theory of Plasma Chromatography Gaseous Electrophoresis - Review. *Anal. Chem.* **1975**, *47* (7), 970–983.

(35) Taraszka, J. A.; Counterman, A. E.; Clemmer, D. E. Gas-phase separations of complex tryptic peptide mixtures. *Fresenius' J. Anal. Chem.* **2001**, *369* (3–4), 234–45.